Flooding of an abandoned fen by beaver led to highly variable greenhouse gas emissions

M. Minke[1,4], A. Freibauer[2], T. Yarmashuk[1,5], A. Burlo[1], H. Harbachova[1,6], A. Schneider[1,7], V. Tikhonov[1], J. Augustin[3]

[1] APB-BirdLife Belarus, Minsk, Belarus
[2] Bavarian State Research Centre for Agriculture, Freising, Germany
[3] Research Area 1 "Landscape Functioning", ZALF e.V., Müncheberg, Germany
[4] current affiliation: Institute of Botany and Landscape Ecology, University of Greifswald, partner in the Greifswald Mire Centre, Greifswald, Germany
[5] current affiliation: Institute for Nature Management of the National Academy of Sciences of Belarus, Minsk, Belarus
[6] current affiliation: United Nations Development Programme Office in Belarus, Minsk, Belarus
[7] current affiliation: Lower nature conservation authority, Brandenburg at the Havel, Germany

SUMMARY

Rewetting by beaver is reported from many European peatlands and especially from Belarus, which harbours vast abandoned peat extraction sites and a large beaver population. We studied how vegetation and exchange rates of carbon dioxide (CO_2), methane (CH_4) and nitrous oxide (N_2O) changed after beaver had rewetted an abandoned drained fen in Belarus. We selected three sites with different vegetation and water levels. One meadow site turned into a nutrient-poor lake that remained virtually free of living vascular plants, released CO_2 and CH_4, and was a moderate source of greenhouse gases (GHG). In another meadow site that became shallowly flooded, the died-off vegetation was quickly replaced by mire plant species and in the second year the site had already become a strong CO_2 sink, a moderate CH_4 source and, as a result, a strong carbon sink and a weak net GHG emitter. The third site was dominated by forbs that died after intermittent flooding and were only slowly and sparsely replaced by wetland species. This site was a strong source of CO_2 and N_2O. Beaver activity can restore a peatland's carbon sink and reduce GHG emissions. However, as for human-induced rewetting, the outcome depends on starting conditions, position and constancy of the water level, and the time needed for establishment of peat forming vegetation.

KEY WORDS: carbon dioxide, methane, peatland, rewetting, transient response

INTRODUCTION

Peat forms and accumulates in places where water saturation leads to persistent anaerobic conditions and incomplete decomposition of dead plant material (Moore & Bellamy 1974). Worldwide, 400 Mha of peatlands contain some 500 Gt of carbon in their peats (Immirzi *et al.* 1992, Joosten 2009, Page *et al.* 2011). Artificial drainage for agriculture, forestry and peat extraction has changed more than 50 Mha of peatlands from long-term carbon sinks into the source of nearly five percent (2 Gt CO_2-eq. per year) of global anthropogenic greenhouse gas (GHG) emissions (Ciais *et al.* 2013, Joosten *et al.* 2016, Leifeld & Menichetti 2018). Therefore, peatland conservation and rewetting are of high importance for climate change mitigation (Joosten *et al.* 2012). Over the last two decades deliberate rewetting has been slow in Europe, which now has 200,000 ha of rewetted peatlands (= 0.7 % of the drained peatland area) (Tanneberger *et al.* 2017).

Beavers are important for water table regulation and rewetting in many peatlands worldwide. They prefer to build their dams in narrow stream channels with grasses, forbs and hardwood vegetation (Gurnell 1998), often raising the water table by several decimetres. The dams create ponds that increase open water area (Morrison *et al.* 2014) and water storage (Woo & Waddington 1990), raise the groundwater table in the vicinity (Karran 2018), and induce succession towards flooding-tolerant vegetation (Mitchell & Niering 1993). In the European part of the Russian Federation 750,000 ha of drained forested peatlands have rewetted spontaneously due to poor maintenance of drains and beaver activity (Sirin *et al.* 2017). After Russia, Latvia, Lithuania and Sweden, Belarus has the fifth largest beaver population in Europe (Halley *et al.* 2012). Belarus also

has 281,500 ha of abandoned peat extraction sites, including a restored area of 21,333 ha (Bambalov *et al.* 2017). Beaver dams have raised the water level in various peatland sites in Belarus (Rakovich & Bambalov 1996, Voitekhovitch *et al.* 2011a, 2011b), including the abandoned milled fen Poplaŭ Moch (Tanneberger & Thiele 2011), a fen polder in the Chernobyl region (Zhuravlev & Tanneberger 2011), and the Jasiel'da River fen of "Sporaŭski zakaznik" Ramsar site (Ilina & Gurova 2016).

Beaver ponds are significant sources of carbon and emission hotspots for methane (CH_4) and carbon dioxide (CO_2) (Roulet *et al.* 1997). CH_4 emissions from beaver ponds are in the upper part of the range for fens (Bartlett & Harriss 1993, cf. Wilson *et al.* 2016), and their sparse plant cover does not sequester sufficient carbon even to compensate for the CO_2 produced by heterotrophic respiration (Roulet *et al.* 1997). Large CH_4 fluxes can also be expected when abandoned peat extraction sites are rewetted by beaver activity and this causes drowning of vegetation that is not tolerant to flooding (Augustin & Chojnicki 2008, Hahn-Schöfl *et al.* 2011, Hahn *et al.* 2015). The overall net carbon and GHG balance of beaver-modified peatlands will depend on the vegetation cover and dynamics.

After beaver were released in a drained valley fen in Scotland, the vegetation shifted from *Urtica dioica* domination towards wetland species within 12 years (Law *et al.* 2017). In a former peat extraction site on the Dakudaŭskaje mire (Belarus), beaver activity facilitated the establishment of wet *Eriophorum vaginatum* - *Sphagnum cuspidatum* vegetation (Voitekhovitch *et al.* 2011a), whereas in the cutover Dalbeniški and Zelikaŭ Moch peatlands rewetting by beaver supported the expansion of a wide range of fen and meadow species including *Carex acuta*, *C. lasiocarpa*, *Eriophorum angustifolium*, *Potentilla anserina*, *Phragmites australis* and *Sphagnum angustifolium* (Rakovich *et al.* 2003, Voitekhovitch *et al.* 2011b).

So far, there has been no systematic study of the effect of beaver-induced rewetting on the carbon and GHG fluxes of formerly drained peatlands. Indeed, such research is challenging because beaver activity cannot be planned. Our study became possible only because an established research location was unexpectedly flooded by beaver, and it captured gaseous carbon fluxes during the most dynamic transition period immediately following the rise of the water table. The objective of this study was to track beaver-induced changes in a fen site that had been prepared but not used for peat extraction, and to better understand the potential for beaver activity to reduce GHG emissions and restore the carbon sink function of abandoned peat extraction sites.

METHODS

Study area

The fen complex "Barcianicha" is situated in central Belarus (Figure 1). The climate is temperate continental and humid, with warm summers (Dfb after Köppen 1936, cf. Kottek *et al.* 2006) and a mean annual precipitation of 665 mm (1979–2008, Valožyn meteorological station, Belgidromet). The first study year (2010/2011) was wetter (total precipitation 740 mm) and the second year (2011/2012) was drier (633 mm) than average, but mean annual temperature was close to the 30-year average (6.4 °C) in both years (6.5 °C and 6.9 °C, respectively). The fen is fed by groundwater. The soil is a Rheic Eutric Fibric Histosol (IUSS Working Group WRB 2015). An area of about 197 ha was drained in 1990 and milled peat extraction was in progress on 149 ha from 1992 to 1995 (Maksimenkov *et al.* 2006).

Figure 1. Locations of the study sites and beaver dam. Photograph by Konstantin Timokhov. Drainage system after Kozulin *et al.* (2010).

At the south-western edge of the fen (54.0937 °N, 26.2868 °E, Figure 1) the vegetation was removed after drainage, but peat extraction did not take place (personal communication, A. Kozulin 2018). The southern part of this area was used for stockpiling whereas its northern part was levelled and, between 1995 and 2007, both were occasionally planted with maize to feed wild boar (personal communication, A. Kozulin 2018). In 2009 the area was still drained with a meadow in the northern part separated by an auxiliary channel from the southern part, which was overgrown by nettles. Probably in the autumn of 2009, beaver blocked the main channel (M-1 in Figure 1).

Two study sites, in meadow and nettles respectively, were selected before beaver activity started in the autumn of 2009. The third study site was in a depression in the meadow where winter floodwater did not disappear in the summer of 2010, signalling that beaver had changed the area's hydrology. Between September 2010 and September 2012, substantial differences in water level and vegetation developed between the study sites (Figures 2 and 3):

1. *Deeply flooded meadow*: formerly *Agrostis stolonifera-Equisetum palustre* meadow, flooded since autumn 2009. Vegetation had completely died off in summer 2010 and emergent macrophytes were still absent in 2012.
2. *Shallowly flooded meadow*, 11 m north of and 35 cm higher than the first site. Water level at the surface since autumn 2009 or winter 2009/10. This site was dominated by *Agrostis stolonifera* and *Potentilla anserina* in summer 2010, and was rapidly colonised by mire species during the study (2010–2012).
3. *Shallowly flooded forbs*: formerly dominated by *Urtica dioica* and *Poa trivialis*, not flooded prior to the measurements. Succession was slow after flooding and only a few *Typha latifolia* plants had established by 2012.

Soil

In July 2010, peat stratigraphy and degree of peat decomposition after von Post (AG Boden 2005) were determined at Sites 2 and 3 using a Russian corer (50 cm long, 5 cm diameter). The top 0–10 cm were

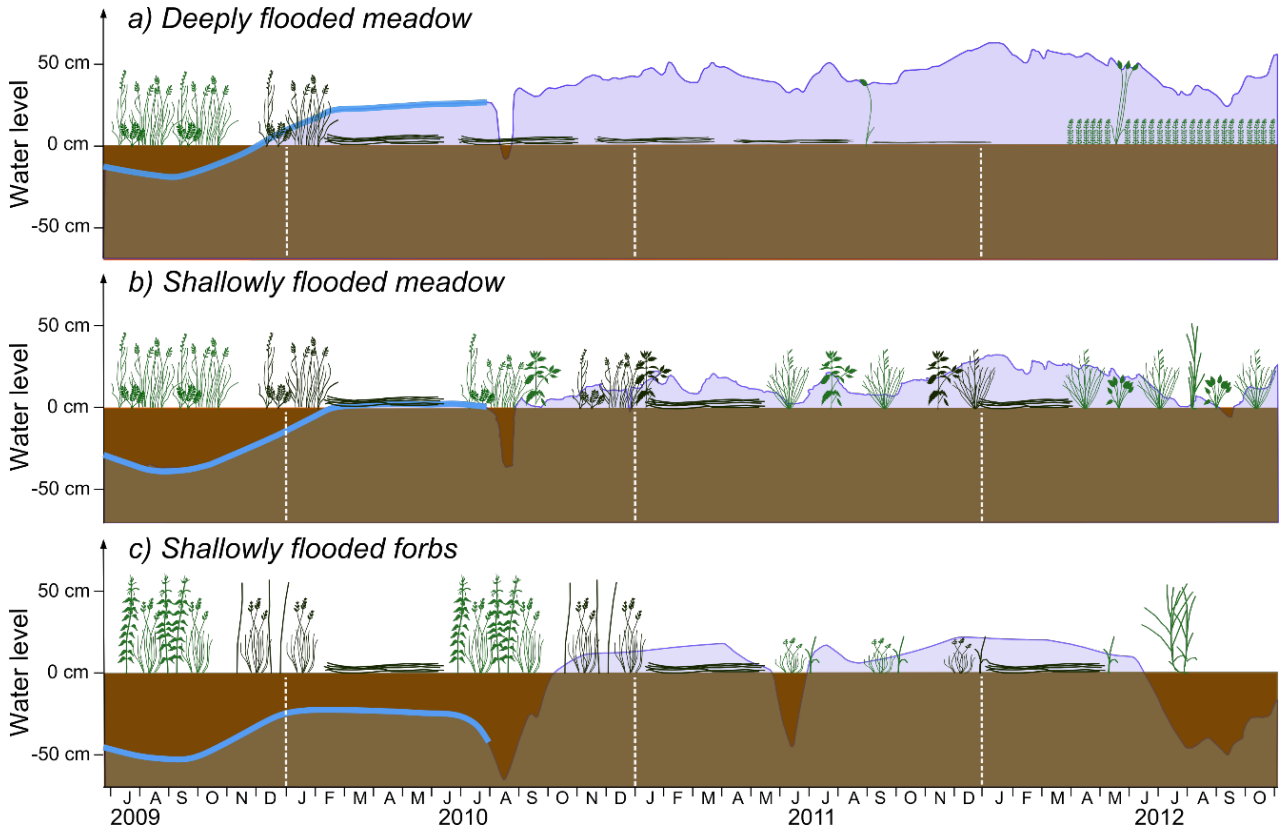

Figure 2. Sketch of water level and vegetation dynamic at the study sites. Water levels before measurements started in August 2010 were derived from visual observations and occasional measurements. Plants are drawn after Succow & Jeschke (1990) and Rothmaler (2000).

analysed for pH (Hanna Combo HI 98130) and total carbon and nitrogen (Vario EL III, Germany) in July 2010 and October 2012, respectively, using three samples per plot taken immediately adjacent to the collars (Table 1).

Water levels

We reconstructed water levels prior to the start of regular measurements using the dominant plant species recorded in June 2009 and photographs taken in June, September and November 2009 and in April and June 2010 (Table 2, Figure 2). From August 2010 to October 2012, water levels relative to ground surface were measured manually at each site every 2–3 weeks using pre-installed perforated tubes. Automated daily water level measurements using a Mini Diver data logger (Eigenbrodt, Germany) were carried out at Site 2 and extrapolated to Site 1 using linear regression ($r^2 > 0.9$). Daily water levels at Site 3 were derived by linear interpolation between the manual measurements because their correlation with the automatically recorded water levels was poor. Annual quantiles (5 % / 50 % / 95 %) of daily water levels were calculated for every plot and averaged per site (Table 2).

Vegetation

The cover of plant species inside the GHG measurement collars (plots; see next section) was assessed in 2010, 2011 and 2012 using cover classes after Peet *et al.* (1998): 1 = very few individuals, 2 = 0–1 % cover, 3 = 1–2 %, 4 = 2–5 %, 5 = 5–10 %, 6 = 10–25 %, 7 = 25–50 %, 8 = 50–75 %, 9 = 75–95 %, 10 ≥ 95 %. Total green plant cover was assessed as a percentage of total cover, at monthly intervals. The vegetation type of each site was named using one dominant and one indicator species from the assessment in summer 2010.

GHG measurements

Each site was equipped with three 70 cm × 70 cm plastic collars arranged in a row ~40 cm apart and inserted into the peat to 15 cm depth. Chamber measurements were conducted over two complete

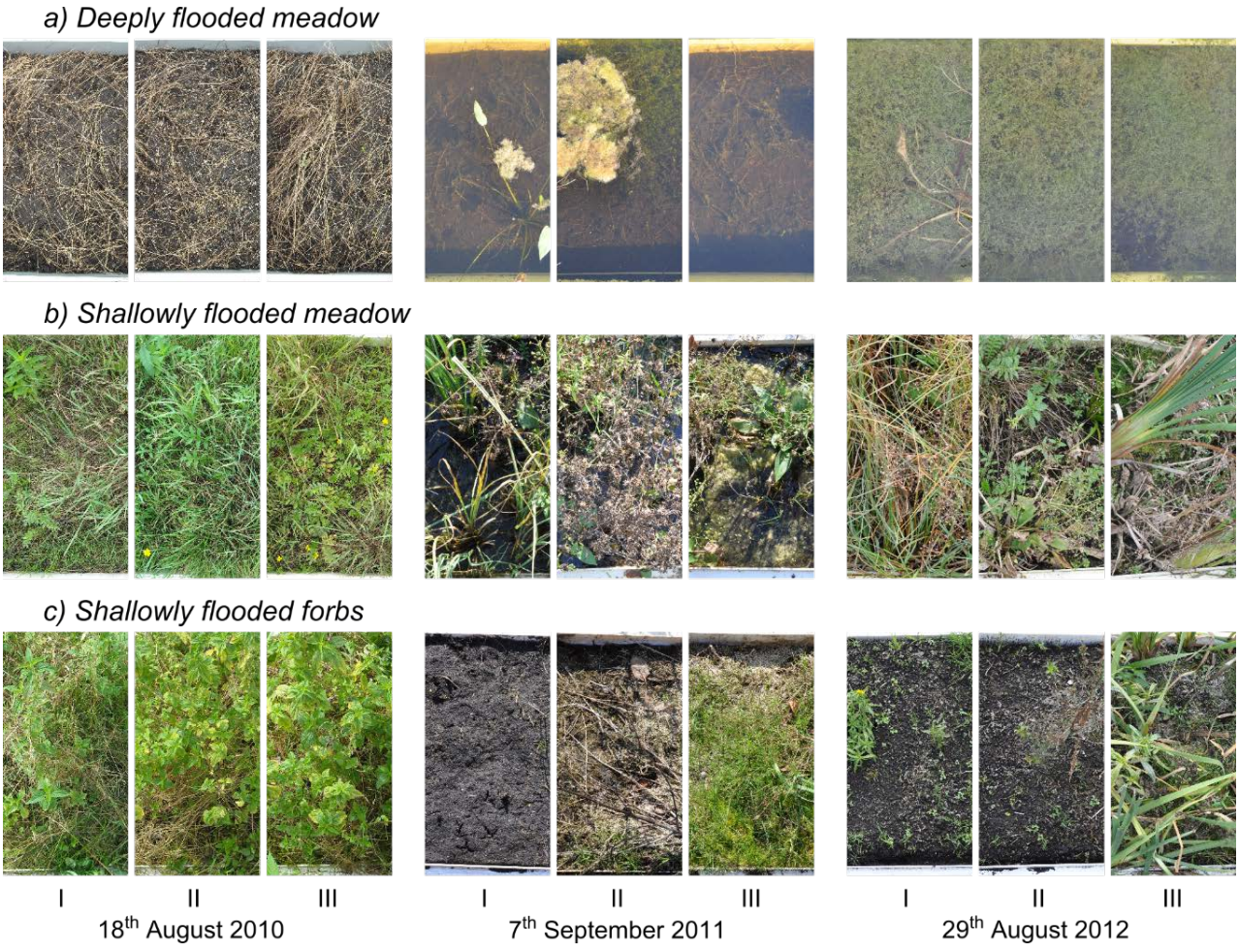

Figure 3. Photograph of the plots at the study sites in 2010, 2011 and 2012. The distance between the upper and lower border of a photograph is 70 cm, equal to plastic collar height.

Table 1. Site characteristics. [a] von Post peat decomposition scale: H3 very slightly, H4 slightly, H5 moderately, H6 moderately highly, H9 practically fully decomposed peat, November 2011. [b] Means ± standard deviations, *n* = 3 plots × 3 samples per plot (pH in July 2010, C_{tot} and N in October 2012).

Site	Profile description (cm below surface)[a]	Surface peat (0 to 5 cm depth)[b]			
		pH	C_{tot} (%)	N (%)	C_{tot}/N
Deeply flooded meadow	0–4 lost, 4–15 H9, 15–25 radicel peat (H5) with wood, 25-36 radicel peat (H5) with *Alnus* wood and gyttja, 36-43 radicel peat (H4) with gyttja, 43-46 *Alnus* wood peat (H3), 46-52 clay gyttja (K2) with wood and radicels, below: sand.	N/D	45.3 ± 1.6	3.0 ± 0.2	15.2 ± 1.0
Shallowly flooded meadow	0–5 lost, 5–20 H9, 20–27 H5 with wood, 27–45 radicel peat (H5) with gyttja and wood, 45–70 radicel peat (H4) with gyttja and wood, 70–83 clay gyttja (K3) with *Alnus* wood, 83–85 transition between gyttja and sand, below: fine sand.	5.7 ± 0.2	44.1 ± 0.4	3.0 ± 0.1	14.8 ± 0.6
Shallowly flooded forbs	0–13 lost, 13–25 H9, 25–40 H6 with radicel peat and wood, 40–55 H5 with *Alnus* wood, 55–80 radicel peat (H4) with wood, 80–88 radicel peat (H4) with gyttja, 88–93 clay gyttja (K3) with *Alnus* wood, 93–94 *Alnus* wood peat (H3), 94–98 clay gyttja (K3), below: middle sand.	6.7 ± 0.1	41.9 ± 1.0	2.9 ± 0.1	14.3 ± 0.3

Table 2. Water levels and [a]annual quantiles (5 % / 50 % / 95 %) of daily water levels (means ± Standard Deviations, *n* = 3 plots).

Site	Water levels (cm above surface)			
	Up to Sep 2009	Autumn 2009 to Aug 2010	Sep 2010 to Aug 2011[a]	Sep 2011 to Aug 2012[a]
Deeply flooded meadow	non-flooded, estimated average 0 to -10	flooded, estimated average 20 to 40	flooded, 36 / 45 / 54 ± 2	flooded, 34 / 54 / 67 ± 2
Shallowly flooded meadow	non-flooded, estimated average -30 to -40	at surface, estimated average -10 to 10	flooded, 2 / 11 / 20 ± 1	flooded, 0 / 20 / 33 ± 1
Shallowly flooded forbs	non-flooded, estimated average -40 to -50	non-flooded, estimated average -30	mostly flooded, -30 / 13 / 19 ± 4	mostly flooded, -49 / 16 / 24 ± 4

years, including winter. Ice cover was removed before measurement if not too thick. Thus, our approach did not track the winter flux dynamics associated with natural closure (no gas efflux) and cracking (high gas efflux) of ice cover (Tokida *et al.* 2007), but recorded winter fluxes when there was no ice, yielding low winter flux estimates that are expected to compare well with total winter emissions when integrated over time.

CO_2 exchange was measured on days with no or little clouds, using cooled transparent and opaque white chambers with internal dimensions 72.5 cm × 72.5 cm × 51.2 cm. Installed fans provided air mixing. If necessary, the chambers were enlarged to accommodate tall plants and/or high water levels. We performed eight to ten transparent chamber measurements of two to three minutes per collar over the daily range of photosynthetically active radiation (*PAR*) to determine the light response of gross primary production (*GPP*), and a similar number of opaque chamber measurements to capture the temperature response of ecosystem respiration (R_{eco}). To account for changes in response curves resulting from changing water table depth and plant development, measurements were repeated every third to fourth week. During chamber closure CO_2 concentration, air temperature and *PAR* were recorded every five seconds (LI-820, LI-COR Biosciences, USA; "109" temperature probes, SKP215, and CR200 or CR1000, Campbell Scientific, USA). Water temperatures at 2, 5 and 10 cm depth were read once per chamber closure (Pro-DigiTemp insertion thermometers, Carl Roth, Germany). Leiber-Sauheitl *et al*. (2015) confirm the reliability of annual R_{eco} models built on clear-day measurements conducted about every third week. Comparing various manual chamber approaches, the 'sunrise approach', as used in our study, was identified to best model annual net CO_2 balances when it covered the entire diurnal range of CO_2 fluxes, *PAR* and temperature (Huth *et al*. 2017).

CH_4 and nitrous oxide (N_2O) fluxes were measured every second week during the snow-free period and monthly during winter using opaque white chambers without fans, which had the same plan area as the CO_2 chambers but were shaped as truncated pyramids. Four to five air samples were taken from the chamber headspace with 60 ml vials during a 15–20 min enclosure, and were subsequently analysed in the laboratory using a gas chromatograph (Chromatec-Cristal 5000.2 with ECD and FID; Chromatec, Russia) and an auto-sampler (Loftfield, Germany). From August 2010 to September 2012, a total of 40 measuring campaigns for CH_4 and N_2O, plus 22 for CO_2, were carried out at each site.

Variables for flux models (air temperature and *PAR*) were recorded on-site during the GHG measurement campaigns and monitored continuously by a climate station in Višnieva, 5.6 km north-west of Barcianicha. Regression between site and climate station temperature data was subsequently applied to derive continuous half-hourly time series for each site.

Flux rate calculation

GHG fluxes were estimated from linear concentration changes in the chambers over time. To determine CO_2 flux rates a moving window of constant length (60 seconds for Sites 2 and 3; 90 seconds for Site 1, where the lack of vascular plants meant that concentration changes were slow) was used to select the regression sequence with maximum R^2, minimum variance, maximum chamber temperature change ≤ 0.75 K and, for transparent chambers at *PAR* > 200 µmol s^{-1}, *PAR* fluctuations below ~10 %. If the maximum R^2 and minimum variance criteria indicated different fluxes (51 % of all flux measurements), the mean of both was used as the flux estimate. CH_4 fluxes were estimated with the R package "flux 0.2–1" (Jurasinski *et al*. 2012). First, all usable flux measurements were identified on the basis of total number of available concentration measurements per chamber closure (minimum three). Then, if the normalised root mean square error (NRMSE) was < 0.2, the flux with the largest number of concentration measurements was preferred. If NRMSE was ≥ 0.2, the flux with the lowest NRMSE was selected. Fluxes ≥ 0 were accepted if NRMSE < 0.4, $R^2 \geq 0.8$ and $n \geq 3$. This was the case for 250 of the 353 CH_4 flux measurements. All other flux measurements were discarded. N_2O flux rates were estimated using the same samples as for CH_4 flux calculation.

Modelling of annual GHG fluxes

Net ecosystem exchange (*NEE*, the net CO_2 flux between the ecosystem and the atmosphere) was modelled plot-wise, to account for plant cover differences among plots (Figure 2, Table A1). Parameters for modelling ecosystem respiration (R_{eco}) were estimated separately for each measurement campaign by fitting dark chamber flux data against air temperature using the respiration function of Lloyd & Taylor (1994):

$$R_{\mathrm{eco}} = R_{\mathrm{ref}} \times \exp\left[E_0 \times \left(\frac{1}{T_{\mathrm{ref}} - T_0} - \frac{1}{T - T_0}\right)\right] \quad [1]$$

where R_{eco} = ecosystem respiration (mg m^{-2} h^{-1}), R_{ref} = R_{eco} at reference temperature (mg m^{-2} h^{-1}), E_0 = activation energy-like parameter (K),

T_{ref} = reference temperature (283.15 K), T_0 = temperature constant for the start of biological processes (227.13 K) and T = air temperature during the measurement of best fit with the dataset (K).

If parameterisation failed or the temperature amplitude was below 3 K, the mean campaign R_{eco} flux was taken as R_{ref} and E_0 was set to zero. This applied to 30 % of the campaigns at Site 2 and to 62 % of campaigns at the other sites. The R_{eco} flux between each pair of measuring campaigns was calculated in 30-minute steps using continuous temperature records and the parameters of both the previous and the subsequent campaign, and taken as the distance-weighted mean of the two resulting flux values.

Gross primary production rates (*GPP*) were determined from measured *NEE* flux rates by subtracting modelled R_{eco} fluxes for the corresponding times. A rectangular hyperbola (Michaelis & Menten 1913) was then fitted to the relationship between *PAR* and *GPP* to obtain *GPP* parameter sets consisting of α (initial slope of the curve), light use efficiency and GP_{max} (maximum rate of carbon fixation at infinite *PAR*) (Drösler 2005, Hoffmann *et al.* 2015).

$$GPP = \frac{\alpha \times PAR \times GP_{\max}}{\alpha \times PAR + GP_{\max}} \quad [2]$$

If no fit could be determined for Equation 2 (10 % of all campaigns), *GPP* was omitted from further calculations. When green plant material and *GPP* fluxes were absent, the parameters α and GP_{max} were set to -0.00000000001. *GPP* fluxes between measuring campaigns were determined in 30-minute steps in the same manner as described for R_{eco} but based on continuously monitored *PAR* data and the appropriate *GPP* parameter pairs.

Finally, annual CO_2 fluxes were derived by integrating the time series from 18 Sep 2010 to 17 Sep 2011 and 18 Sep 2011 to 17 Sep 2012, and calculating *NEE* as the difference between *GPP* and R_{eco}:

$$NEE(\mathrm{CO_2}\ \text{balance}) = GPP + R_{\mathrm{eco}} \quad [3]$$

Annual CH_4 emissions from Site 1 were modelled using Lloyd & Taylor fits between CH_4 fluxes and mean daily water temperature (Equation 1, cf. Minke *et al*. 2016). This was done site-wise because plot-wise parameter fits were not significant for most years and plots. Site-wise modelling is justified on the basis of the high similarity in soil characteristics and water levels among the plots.

CH_4 emissions from Site 2 could not be modelled adequately by Equation 1, probably because the water level sometimes dropped to the soil surface, causing the CH_4 flux (CH_4) to decrease. Instead we used a site-wise multiple regression function combining daily water temperature (T_w) and the average water level of the past 30 days (WL_{30}), where $b0$ is the basal ln(CH_4 flux + 1) and $b1$ and $b2$ are coefficients for the explanatory variables:

$$\ln(CH_4 + 1) = b0 + b1 \times T_{\mathrm{w}} \times WL_{30} \quad [4]$$

It was not possible to model the strongly dynamic CH_4 emissions from Site 3 using the environmental data recorded. Therefore, annual CH_4 emissions from this site were estimated by plot-wise linear interpolation. Annual N_2O emissions could not be modelled for any of the sites on the basis of the environmental data, and these were estimated by plot-wise linear interpolation.

The carbon balance was calculated as:

$$C\ balance = NEE(C) + CH_4(C) \quad [5]$$

and the GHG balance was calculated assuming global warming potentials of CO_2, CH_4 and N_2O for a time horizon of 100 years (Myhre *et al.* 2013):

$$GHG\ balance = 1 \times NEE(\mathrm{CO_2}) + 28 \times CH_4 + 265 \times N_2O \quad [6]$$

Precision of flux rate calculation and model performance

The performance of empirical CO_2 and CH_4 models (except for the linear models) was evaluated by plot-wise and year-wise calculation of Nash-Sutcliffe efficiency (NSE; Moriasi *et al.* 2007), which indicates how well a comparison of observed versus modelled data fits the 1:1 line. NSE was first calculated for all modelled fluxes versus all measured fluxes to assess the calibration quality. Then, to evaluate the predictive accuracy of the model, the calculation was repeated iteratively, leaving out each measurement campaign in turn and calculating NSE for all remaining modelled fluxes versus the measured fluxes of the left-out campaign (leave-one-out cross-validation, cf. Hoffmann *et al.* 2015).

Errors of the modelled annual CO_2 fluxes were calculated using Monte Carlo simulation in four steps. First, temperature uncertainty was quantified by calculating bootstrap temperature transfer functions based on re-sampling site and (Višnieva) station temperature pairs 200 times. Second, bootstrap R_{eco} parameter pairs were produced by re-sampling the residuals of the R_{eco} fits 200 times

(Efron 1979, Leiber-Sauheitl *et al.* 2014). If R_{eco} parameterisation was not successful, E_0 was set to zero and bootstrap R_{ref} values were derived by re-sampling the measured R_{eco} fluxes 200 times. Third, each R_{eco} bootstrap parameter pair was combined with a bootstrap temperature transfer function and 200 annual R_{eco} models were calculated per plot. Fourth, up to 200 *GPP* fluxes were created from each measured *NEE* by subtracting the bootstrap R_{eco} values that corresponded to them in time. The residuals of the 200 derived *GPP* fits were re-sampled 200 times, but on average only 38 % of the bootstrap fits were successful. The resulting 200 × 76 *GPP* parameter pairs were used to construct about 15,200 annual *GPP* and *NEE* models per plot. Quantiles (95 % and 5 %) and standard errors were calculated from all bootstrapped R_{eco}, *GPP* and *NEE* models.

Errors of annual CH_4 fluxes from Site 1, which was modelled using the Lloyd & Taylor respiration function (Equation 1), were estimated by a similar method to the one used for R_{eco} but re-sampling 5,000 times and including the uncertainty of the measured fluxes, resulting in 5,000 annual CH_4 models. Error estimation for annual CH_4 emissions from Site 2 (Equation 4) was conducted as follows. First, temperature and water level uncertainties were quantified by bootstrapping transfer functions between site and station/logger pairs, re-sampling 5,000 times. Second, *rnorm* (R 3.1.1) was used to generate a set of 5,000 normally distributed flux values for every flux measurement, based on estimated CH_4 flux rates and their standard deviation. Third, each of the 5,000 water temperature and water level datasets was paired with one of the 5,000 flux datasets, and each derived dataset was then re-sampled 5,000 times resulting in a total of 25,000,000 multiple regression fits and corresponding parameter trios (*b0*, *b1* and *b2* in Equation 4) per year. Finally, 5,000 parameter trios were randomly sampled, then combined with the 5,000 soil temperature and water level datasets to calculate 5,000 annual CH_4 models.

Estimation of the uncertainty of linear models (N_2O from all sites, CH_4 from Site 3) was based on uncertainty of measured fluxes. 40,000 normally distributed values of each flux were generated using *rnorm* and subsequently linearly interpolated. To estimate the site-wise uncertainty of linear models for each time step, the 40,000 plot-wise generated values were combined site-wise by calculating the mean of the first values generated from the three plots, continuing with the second, and finishing with the 40,000th. Site-wise (rather than plot-wise) model uncertainties are shown in the timelines of linear models to improve readability (Figure 4).

Site-level annual fluxes, of CH_4 from Site 3 and of CO_2 and N_2O from all study sites, were derived as the arithmetic means of the annual plot values. The standard errors of these means indicate their precision, which is a function of number of plots, differences among plots, and uncertainties of annual flux estimates. For Sites 1 and 2, annual CH_4 fluxes and their uncertainties were calculated directly at site level.

RESULTS

The peat on all sites consisted of a 15–25 cm highly decomposed top layer, followed by 20–60 cm of moderately decomposed radicel peat with some wood, which was underlain by few centimetres of clay gyttja, followed by sand (Table 1). The surface peat (pH 5.7–6.7, C/N 14.3–15.2) was subneutral to alkaline and eutrophic - moderately rich (after Succow *et al.* 2001).

In June 2009, the vegetation at Sites 1 and 2 was similar. The dominant plant species were *Agrostis stolonifera* and *Potentilla anserina*, which are typical for moist and wet but not permanently flooded soils (water level fluctuating between 10 cm above and 45 cm below surface) and mesotrophic to eutrophic conditions (Koska *et al.* 2001). Until September 2009 the water level at both of these (meadow) sites probably oscillated between a few centimetres and a few decimetres below surface (Table 2, Figures 2a and 2b).

Deeply flooded meadow (Site 1)

Water level and vegetation

Site 1 became flooded no later than November 2009, indicating that the southern main channel was already blocked by a beaver dam. The water level rose to 20–40 cm above surface. Regular monitoring started in August 2010 and showed a short-term drop in water level (15 to 28 August), probably because the beaver dam was temporarily leaky (Figures 2a, 3a and 4a). Then the water level rose again and remained fairly stable at ~50 cm (90 % confidence interval ~35–60 cm) above surface throughout the GHG measurement period (Table 2). Above- and below-ground biomass died after flooding and dead plant material covered the site in 2010 and 2011 (Figures 2a and 3a). In 2012 the site was colonised by *Chara vulgaris*, indicating mesotrophic and alkaline conditions (Koska *et al.* 2001). No emergent plants established after rewetting except for few individuals of *Alisma plantago-aquatica* (Table A1). Total green vascular plant cover remained below 1 % (Figure 4b).

CO_2 balance

Annual balances hardly differed among plots and years, and showed the site to be a net source of CO_2-C (141 ± 3 g m^{-2} yr^{-1} and 143 ± 12 g m^{-2} yr^{-1} in the first and second years, respectively).

The calibration tests revealed good performance of the CO_2 models (NSE 0.59–0.67), but their predictive accuracy was acceptable only in the second year (Table A2). CO_2 exchange of the site was driven almost entirely by heterotrophic respiration. *GPP* amounted to small CO_2-C fluxes of -30 ± 14 g m^{-2} yr^{-1} in the second year only, and was certainly related to the spreading of *Chara vulgaris* (Figures 4c and 5a, Table 3).

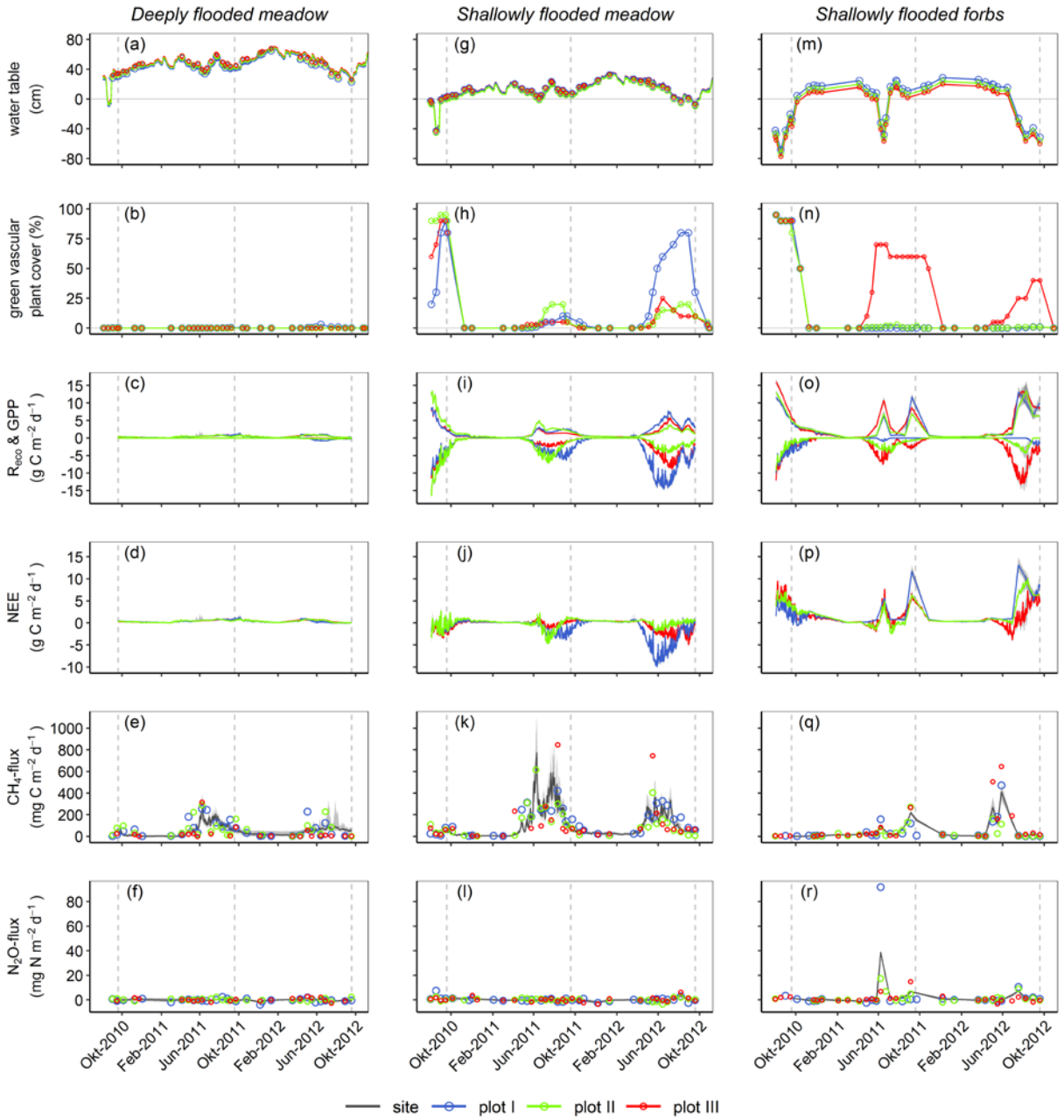

Figure 4. Water table position (a, g, m) green plant cover (b, h, n), mean daily *GPP* and R_{eco} (c, i, o), *NEE* (d, j, p), CH_4 (e, k, q) and N_2O fluxes (f, e, r). Points indicate measured values (grey = plot I, white = plot II, black = plot III), lines show modelled or interpolated values (solid-black = site, solid-grey = plot I, dotted-grey = plot II, dashed-grey = plot III). Shading depicts 90 % confidence intervals. CO_2 fluxes were modeled plot wise, CH_4 fluxes from *deeply flooded meadow* and *shallowly flooded meadow* were modelled site wise. CH_4 fluxes from *shallowly flooded forbs* and N_2O fluxes from all sites were interpolated plot-wise linearly, but shown with their confidence intervals site-wise to improve vividness. Vertical dashed lines mark start and end of periods integrated to annual GHG emissions.

N_2O and CH_4

Emissions of N_2O were just above zero in the first year and below zero in the second year (Figures 4f and 5c). CH_4-C fluxes were 18 ± 3 and 15 ± 4 g m^{-2} yr^{-1} (Table 3, modelled annual site flux ± SE). Emission rates were driven by temperature. Model performance was acceptable, but better in the first year than in the second year (Table A2). Modelled annual CH_4 fluxes were 10 % lower in the first year, and 25 % higher in the second year, than annual fluxes calculated by linear interpolation.

Carbon and GHG balance

Plant succession was slow and the site remained a moderate source for carbon (C) (159 ± 4 and 158 ± 12 g m^{-2} yr^{-1} in the first and second years, respectively, Table 3, site mean ± SE) and GHG (CO_2 equivalent values of 12.0 ± 1.1 and 10.4 ± 1.7 t ha^{-1}, respectively, Table 4). 46 % of the GHG emissions resulted from CO_2 and 54 % from CH_4, while N_2O fluxes were zero. The GHG emissions were within the IPCC (2014) range for rewetted temperate fens.

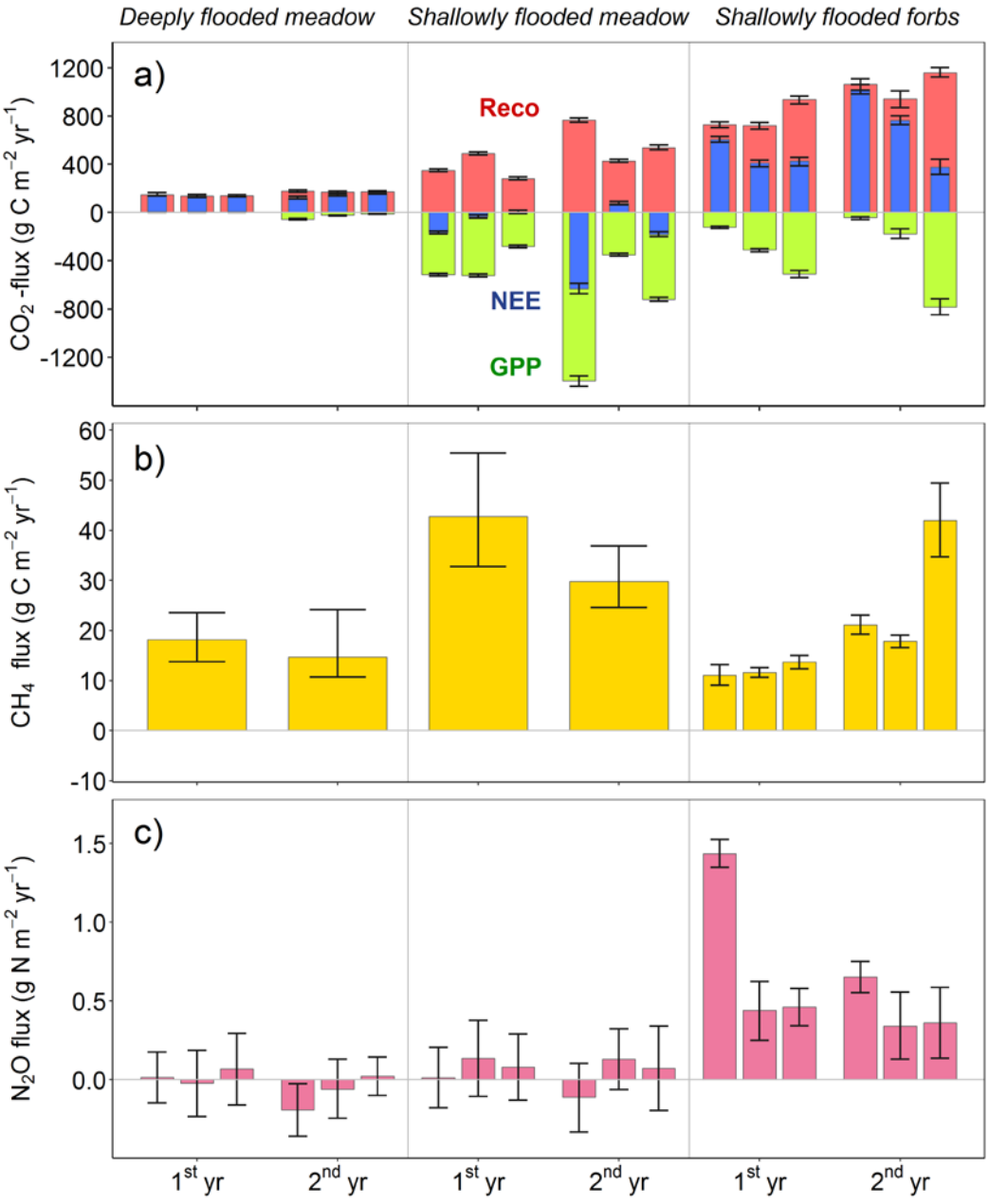

Figure 5. Annual CO_2 (*NEE*, R_{eco}, *GPP*), CH_4 and N_2O fluxes (a, b, c). Fluxes are given plot-wise, except for CH_4 fluxes from *deeply flooded meadow* and *shallowly flooded meadow* that were modelled site-wise. Error bars represent 90 % confidence intervals. Plots are ordered I, II, III.

Table 3. Annual *NEE*, R_{eco}, *GPP* and CH_4 (all as C-eq), N_2O (as N-eq) and C balance. The values given are means ± Standard Error, n = 3 plots except: [a] annual CH_4 emissions for both *meadow* sites are modelled site-wise and Standard Errors calculated by bootstrapping; and [b] Standard Errors of annual C balance are calculated by error propagation (square root of the sum of the squared SEs of CO_2 and CH_4 fluxes).

Site	Year	*NEE* (g m^{-2} yr^{-1})	R_{eco} (g m^{-2} yr^{-1})	*GPP* (g m^{-2} yr^{-1})	CH_4 [a] (g m^{-2} yr^{-1})	N_2O (g m^{-2} yr^{-1})	C [b] (g m^{-2} yr^{-1})
Deeply flooded meadow	1	141 ± 3	141 ± 3	0	18 ± 3	0.01 ± 0.04	159 ± 4
	2	143 ± 12	173 ± 3	-30 ± 14	15 ± 4	-0.06 ± 0.05	158 ± 12
Shallowly flooded meadow	1	-66 ± 52	373 ± 61	-439 ± 80	43 ± 7	0.08 ± 0.03	-23 ± 52
	2	-245 ± 207	577 ± 100	-823 ± 306	30 ± 4	-0.02 ± 0.05	-216 ± 207
Shallowly flooded forbs	1	482 ± 63	795 ± 71	-313 ± 113	12 ± 1	0.97 ± 0.38	494 ± 63
	2	721 ± 188	1055 ± 63	-334 ± 228	27 ± 8	0.57 ± 0.11	748 ± 188

Table 4. GHG balances (as CO_2-eq) based on the global warming potentials of CO_2, CH_4 and N_2O for a time horizon of 100 yr (GWP_{100} of CO_2 = 1, of CH_4 = 28 and of N_2O = 265 CO_2 equivalents, Myhre *et al*. 2013). The values given are means ± Standard Error, n = 3 plots except: [a] annual CH_4 emissions for both *meadow* sites are modelled site-wise and Standard Errors calculated by bootstrapping; and [b] Standard Errors of GHG balance are calculated by error propagation (square root of the sum of the squared SEs of the CO_2, CH_4, and N_2O fluxes). [c] Maximum possible uncertainty from campaign frequency and temporal interpolation.

Site	Year	CO_2 flux (t ha^{-1} yr^{-1})	CH_4 flux [a] (t ha^{-1} yr^{-1})	N_2O flux (t ha^{-1} yr^{-1})	GHG balance [b] (t ha^{-1} yr^{-1})
Deeply flooded meadow	1	5.2 ± 0.1 (4.9 to 5.8)[c]	6.8 ± 1.1	0.1 ± 0.2	12.0 ± 1.1
	2	5.3 ± 0.4 (4.4 to 6.0)[c]	5.5 ± 1.6	-0.2 ± 0.2	10.5 ± 1.7
Shallowly flooded meadow	1	-2.4 ± 1.9 (-4.0 to -1.0)[c]	16.0 ± 2.6	0.3 ± 0.1	13.9 ± 3.2
	2	-9.0 ± 7.6 (-10.3 to -5.3)[c]	11.1 ± 1.4	-0.1 ± 0.2	2.0 ± 7.7
Shallowly flooded forbs	1	17.7 ± 2.3 (12.1 to 23.3)[c]	4.5 ± 0.3	4 ± 1.6	26.2 ± 2.8
	2	26.4 ± 6.9 (22.9 to 31.7)[c]	10.1 ± 2.8	2.4 ± 0.4	38.9 ± 7.5

Shallowly flooded meadow (Site 2)

Water level and vegetation

Blocking of the main channel by beavers in autumn 2009 resulted in only very shallow flooding at Site 2 because it was 35 cm higher than Site 1. Above-ground plant parts died in winter 2009 and grew again in summer 2010. The vegetation was classified in 2010 as *Agrostis stolonifera* - *Equisetum palustre* - weed (Table A1). The water level rose in October 2010 and remained above the ground surface, by 11 (2–20) cm in 2010/2011 and 20 (0–33) cm in 2011/2012 (Table 2, Figures 2b and 4g). Species not adapted to wet conditions were disappearing gradually until summer 2012. Wetland macrophytes including *Alisma plantago-aquatica*, *Juncus articulatus* and *Carex rostrata* established in summer 2011 and their cover increased in 2012 (Table A1). The first *Typha latifolia* shoot was noted at Plot III in June 2012. Maximum green vascular plant cover was 90–95 % in 2010, 10–20 % in 2011 and 20–80 % in 2012, with the 80 % cover on Plot I in 2012 formed by *Carex rostrata* (Figures 3b, 4h).

CO_2 and carbon balance

Site 2 was a net CO_2 sink in both years. Mean annual *NEE* (as CO_2-C) was -66 ± 52 g m^{-2} yr^{-1} in Year 1 and -245 ± 207 g m^{-2} yr^{-1} in Year 2 (Table 3). The CO_2 models performed well in the calibration test (NSE 0.92–0.98, Table A2). Leave-one-out cross-validation indicated acceptable predictive accuracy (NSE 0.07–0.44) except for one R_{eco} model (NSE -0.04, Table A2). *GPP* (as CO_2-C) was -439 ± 80 g m^{-2} yr^{-1} in the first year and -823 ± 306 g m^{-2} yr^{-1} in the second year, while annual R_{eco} (also as CO_2-C) was only 373 ± 61 and 577 ± 100 g m^{-2} yr^{-1}. Accordingly, GPP/R_{eco} was -1.2 in the first year and -1.4 in the second year, indicating very low heterotrophic respiration and a net accumulation of biomass in the ecosystem. This finding is supported by the very strong correlation between daily R_{eco} and green vascular plant cover (Figure 6) and the increase in vegetation cover.

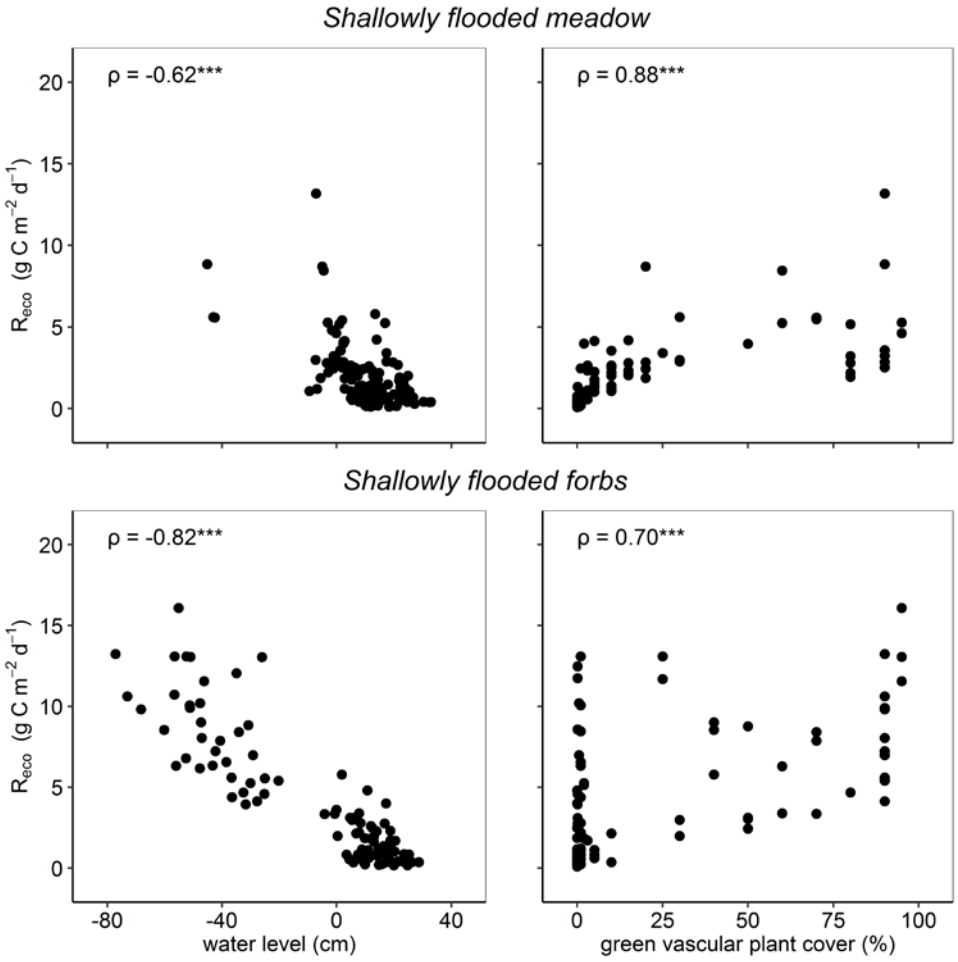

Figure 6. Scatter plot with two-tailed Spearman's rank correlations ρ of recorded water levels and green vascular plant cover with modelled daily rates of R_{eco} of *shallowly flooded meadow* (at the top) and *shallowly flooded forbs* (at the bottom).

N_2O and CH_4

Emissions of N_2O were just above zero in Year 1 and below zero in Year 2 (Figures 4l and 5c). CH_4-C emissions were 43 ± 7 g m^{-2} yr^{-1} in the first and 30 ± 4 g m^{-2} yr^{-1} in the second year (Table 3, Figure 5b). These emissions were driven by temperature and water level. Model performance was acceptable for both years (Table A2). Modelled annual CH_4 emissions in the first year were equal to, and in the second year 6 % below, estimates derived by linear interpolation.

Carbon and GHG balance

On the basis of net CO_2 and CH_4 fluxes, Site 2 was a small net carbon sink of 23 ± 52 g m^{-2} yr^{-1} in the first year and 216 ± 207 g m^{-2} yr^{-1} in the second year. GHG emissions (as CO_2 eq) decreased from 13.9 ± 3.2 t ha^{-1} yr^{--1} in Year 1 to 2.2 ± 7.7 t ha^{-1} yr^{-1} in Year 2 because of increasing CO_2 uptake, decreasing CH_4 emissions and negligible N_2O fluxes. The GHG emissions were again within the IPCC (2014) range for rewetted temperate fens.

Shallowly flooded forbs (Site 3)

Water level and vegetation

In the summers of 2009 and 2010 Site 3 was dominated by *Urtica dioica* and *Poa trivialis*, which are adapted to a wide gradient of site conditions ranging from moderately dry to very moist (water level 5–85 cm below surface), from mesotrophic to polytrophic, and from subneutral to alkaline (Koska *et al.* 2001, Couwenberg *et al.* 2011). The vegetation was classified as *Urtica dioica* - *Galeopsis tetrahit* - weed in 2010. Ditch blocking by beaver in autumn 2009 did not immediately cause flooding at Site 3 but did affect the water level, which suddenly dropped and subsequently recovered in August 2010, as at the two meadow sites (Figure 2). The water level rose in October 2010 and was on average 13 and 16 cm above surface in 2010/2011 and 2011/2012, respectively (Table 2). *Urtica dioica* died during winter 2010/2011. Only Plot III was green in April 2011, covered by small *Poa trivialis*. It must be noted that Plot III was 5 cm higher than Plot II and 9 cm higher than Plot I, with correspondingly lower water levels (Figure 4m). When the water level dropped to 30 cm below surface in summer 2011, the *Poa trivialis* at Plot III recovered, achieved up to 70 % cover, and survived until October 2011 despite subsequent flooding (Figures 2c, 3c and 4n). A small *Typha latifolia* shoot appeared at Plot III in August 2011, grew up in May 2012, and formed ten shoots up to one metre tall in late summer. Although the water level dropped to 50 cm below surface in summer 2012, *Poa trivialis* did not recover that year. Instead, *Typha latifolia* and *Bidens frondosa* dominated Plot III and reached a green vascular cover of up to 40 %. Plots I and II remained bare in 2011 and 2012, although some *Alisma plantago-aquatica* and *Bidens frondosa* plants established at Plot II in summer 2012.

CO_2 and carbon balance

Site 3 was a substantial net CO_2-C source of 482 ± 63 g m^{-2} yr^{-1} in Year 1 and 721 ± 188 g m^{-2} yr^{-1} in Year 2. Calibration tests indicated good performance of the CO_2 models, but predictive accuracy was acceptable for the second year only (Table A2). *GPP* as CO_2-C was -313 ± 113 and -334 ± 228 g m^{-2} yr^{-1} in the first and second years, respectively. Annual R_{eco} was much higher (795 ± 71 and 1055 ± 63 g m^{-2} yr^{-1}), making GPP/R_{eco} -0.4 and -0.3, which suggests a very strong contribution of heterotrophic respiration. Other indications that ecosystem respiration was to a large extent heterotrophic are the coincidence of large R_{eco} fluxes with low plant cover and stronger correlation between daily R_{eco} and water level than between daily R_{eco} and green vascular plant cover (Figure 6).

N_2O and CH_4

High N_2O-N emissions of 0.97 ± 0.38 g m^{-2} yr^{-1} in the first year and of 0.57 ± 0.11 g m^{-2} yr^{-1} in the second year (Table 3) were observed. Emissions occurred during dry periods with water levels below or near the soil surface. Emissions peaked at 40 mg m^{-2} d^{-1} in June 2011 and 7 mg m^{-2} d^{-1} during June–August 2012 (Figures 4m and 4r).

Annual CH_4-C emissions were 12 ± 1 g m^{-2} yr^{-1} in the first and 27 ± 8 g m^{-2} yr^{-1} in the second year (mean of plots ± SE). High CH_4 fluxes were observed in spring and summer (Figure 4q). CH_4 emissions usually decreased when the water level dropped to or below ground surface.

Carbon and GHG balance

Net release of gaseous carbon was high in the first year (494 ± 63 g m^{-2} yr^{-1}) and even higher in the second year (748 ± 188 g m^{-2} yr^{-1}; Table 3). The site was a strong GHG (CO_2 eq) emitter in both years (26.2 ± 2.8 and 38.9 ± 7.5 t ha^{-1} yr^{-1}, respectively; Table 4), with CO_2 contributing 68 %, CH_4 22 % and N_2O 10 %. Total GHG emissions were comparable to those of temperate, deep-drained, nutrient-rich grassland fens (IPCC 2014), but were derived from anaerobic and aerobic mineralisation of litter and peat. This transient hotspot is not yet taken into account in GHG inventories, but it is also very difficult to monitor.

DISCUSSION

Precision and predictive accuracy of annual GHG balances

The low uncertainties of plot-wise annual *NEE* (Figure 5a) indicated high precision of the CO_2 models. The calibration tests confirmed good agreement of modelled CO_2 exchange rates with measured fluxes (Table A2). However, the predictive accuracy of *NEE* models tested by leave-one-out cross validation was, in part, low. This means that the parameterisation of the R_{eco} and *GPP* response curves changed significantly between measurement campaigns, hampering temporal interpolation. This finding does not compromise the robustness of the annual carbon balances as it was to be expected at our sites for several reasons. First, vegetation cover and phenology of the species varied strongly between measurement campaigns, in particular at Site 3 (*shallowly flooded forbs*) (e.g. Figures 3, 4b, 4h and 4n). On average, 81 % of *GPP* fits were successful. In the remainder *GPP* was too low or saturated quickly with increasing *PAR*. Secondly, the R_{eco} temperature response was buffered by the standing water. Consequently, R_{eco} fluxes often lacked any diurnal temperature response. The proportion of successful Lloyd Taylor fits increased from the first to the second year; from 36 % to 42 % for Site 3, from 60 % to 79 % for Site 2 (*shallowly flooded meadow*), and from 33 % to 39 % for Site 1 (*deeply flooded meadow*).

To get an idea of the largest possible uncertainty in annual *NEE* related to campaign frequency, the model was run n times, leaving out one campaign from each run. The largest and smallest annual *NEE* estimates per plot and year indicate the largest possible error range by temporal interpolation between measurement campaigns (Table 4). The estimated uncertainties were comparable to the spatial variety of the sites (Table 4) and to the uncertainties of annual *NEE* fluxes in peatlands reported from other chamber studies (Samaritani *et al.* 2011, Elsgaard *et al.* 2012, Wilson *et al.* 2013, Beyer *et al.* 2015, Günther *et al.* 2015.).

The CH_4 emission models for Sites 1 and 2 performed well (Table A2). Their robustness was supported by the derivation of similar annual fluxes using linear interpolation. The confidence intervals for the plot-wise annual emissions from Site 3 (Figure 5b) reflect uncertainty of the chamber flux estimates only. Annual estimates could not be tested for predictive accuracy. They ranged between CH_4 emissions from Sites 1 and 2 what is plausible because of higher gross primary production as compared to Site 1 and less stable flooding as compared to both sites (Tables 2, 3).

Annual N_2O fluxes are commonly derived from manual chamber measurements by linear interpolation of fortnightly measurements. The average contributions of N_2O emissions to the GHG balance were 15 % and 6 % in the first and second years, respectively, for Site 3 and below 1 % for Sites 1 and 2.

Three patterns of transient response to flooding by beaver

We found that vegetation type before flooding and water level development determined the pathway of vegetation change and GHG emissions. We derived three response patterns, representing three contrasting situations of the mosaic of vegetation and elevation / depth of flooding in the research area.

1) *Deeply flooded moderately rich moist meadow forms a nutrient-poor lake after one year and remains a moderate carbon and GHG source*.
The meadow was flooded (20–40 cm) in the year before observation and plants did not recover after winter. The water level had been raised to 50 cm above surface at the start of measurements and the site remained more or less free of higher vegetation throughout the study period, confirming the observations of Kozulin *et al.* (2010) and Thiele *et al.* (2011) that colonisation of rewetted fens by helophytes is impeded when the water level is more than 30 cm above surface all year round. *Chara* development indicated that the nutrient supply from groundwater discharge was low, which is an important factor in avoiding eutrophication (Lamers *et al.* 2002). Persistent CO_2 and CH_4 emissions indicate continuing anaerobic decay over two consecutive years, fuelled by dead roots and litter, and most probably partly from peat.

Succession towards helophytes is similarly retarded in the deeply flooded areas that form in restored fens and bogs, for example in depressions previously created by subsidence or peat extraction. GHG emissions, and especially CH_4 fluxes, differ greatly among such areas. Much higher CH_4-C fluxes than in our study (190–370 g m^{-2} yr^{-1} compared to 18 and 15 g m^{-2} yr^{-1}) have been reported from flooded formerly deeply drained fen grassland (Augustin & Chojnicki 2008, Hahn *et al.* 2015), and lower ones (1.5 g m^{-2} yr^{-1}) from flooded bog heath (Drösler 2005). The differences are related to different availability of easily degradable biomass (cf. Hahn-Schöfl *et al.* 2011). Plant biomass was not monitored at our study site, but due to a shorter drainage and cultivation history and because of groundwater instead of surface water supply, both drowned plant biomass and biomass productivity after flooding were certainly lower at the study site as compared to the mentioned rewetted fens.

2) *Shallowly flooded moderately rich moist meadow rapidly turns into sedge fen, a net carbon sink and a moderate to neutral GHG source*.

At Site 2, the meadow still existed in summer 2010 when measurements started, despite beaver activity and rising water levels since autumn 2009. The site then became shallowly flooded (10–20 cm). Most species did not recover in spring 2011 and were replaced by wetland macrophytes. Substantial *GPP* and moderate R_{eco} indicate the formation of new biomass and a subhydric litter layer, part of which might form new peat in the future.

The rewetting situation agreed well with recommended fen restoration practices and was optimal for the recovery of potentially peat-forming species (Timmermann *et al.* 2006, Thiele *et al.* 2011, Zerbe *et al.* 2013). If the water table had not been raised above the surface, but only up to few centimetres below it, the transition to mire vegetation might have been more gradual and CH_4 emissions smaller, because less litter would decay anaerobically and the presence of an aerobic layer would facilitate oxidation of CH_4 (Patterson *et al.* 2007, Drösler *et al.* 2008). CH_4-C fluxes were lower than from a rich fen grassland during the first two years after similar shallow flooding (43 and 30 g m^{-2} yr^{-1} compared to 53 and 98 g m^{-2} yr^{-1}; Meyer 1999).

3) *Shallowly flooded moderately rich moist forbs slowly turn into fen vegetation and remain a strong GHG source for years*.

Most of the vegetation at Site 3 died after shallow flooding (10–20 cm) and succession towards wetland macrophytes took place only at elevated spots. Water level fluctuations with prolonged drawdown (-30 to -50 cm) during dry periods in summer, a large amount of decaying biomass and slow establishment of wetland vegetation turned the site into a large GHG source. *Typha latifolia* may in future colonise larger parts of the forbs area (Gelbrecht *et al.* 2008), but this will not automatically turn the site into a net CO_2 sink (Günther *et al*. 2015, Franz *et al*. 2016; but cf. Strachan *et al*. 2015).

Beaver activity failed to keep the forbs area wet throughout the year, which would be essential to minimise peat mineralisation (Moore & Dalva 1993). It is often difficult to eliminate seasonal water level fluctuations in rewetted fens because of increased evapotranspiration during dry summers (Dietrich & Kaiser 2017), and natural sedge fens can be net CO_2 sinks even though aeration of the upper peat occurs periodically (Dušek *et al*. 2012). However, the water level drawdown at Site 3 was extreme and seemed to be caused by leakage of the beaver dam. Leakage or abandonment of beaver dams put the sustainability of rewetting at risk.

Systematics and mechanisms of response patterns

As discussed above we did not find a uniform response, in terms of vegetation and GHG emissions in the research area, during the first two years after flooding instigated by beaver activity. Slight differences in water table and vegetation between the three sites led to three contrasting response patterns, carbon and GHG effects.

As the response patterns in the transient phases immediately after rewetting agree with patterns of water table - vegetation interactions and carbon and GHG balances in long-term stable situations we can define the development pathways and GHG consequences after rewetting of the fen as follows:

1. After beaver-induced rewetting, the original vegetation dies quickly and is replaced by mire species if the area becomes continuously flooded. Shallow flooding promotes a rapid and robust establishment of mire macrophytes if suitable seed banks are present in the vicinity. Deep flooding hampers the establishment of mire macrophytes. Intermittent flooding stresses the original vegetation and slows down the establishment of new mire vegetation.
2. In the first two years after beaver-induced rewetting CO_2 and CH_4 emissions dominate the GHG response pattern. Vegetation and water level determine the amount and quality of carbon accumulation in newly-formed biomass and the intensity of aerobic decomposition of plant debris and peat, and thus drive the CO_2 balance and CH_4 fluxes. Fluctuating water level with summer drawdown is associated with strong net CO_2 and N_2O emissions. Surprisingly, the CH_4-C emissions we observed were not extremely high, comparing well with emissions from temperate-zone sedge fens (31.2–58.5 g m^{-2} yr^{-1}; Bartlett & Harris 1993, Dise & Gorham 1993, Wickland *et al.* 2001) and from other parts of the Barcianicha fen that were rewetted ten years previously (21.5 g m^{-2} yr^{-1}; Minke *et al.* 2016). This could be explained by low productivity and a limited biomass pool (perhaps associated with a low-nutrient groundwater supply) at this fen, and the situation may be different in fens that were used intensively for agriculture before rewetting and/or in those flooded with nutrient-rich surface water.
3. In the early years after beaver-induced rewetting the fen remains a net carbon source if the water level is not stable but, instead, periodically drops far below the peat surface. It will also be a net carbon source if continuous deep flooding eliminates vascular plants. In this case it could remain a persistent carbon source, as reported from

deep beaver ponds by Roulet *et al.* (1997), or be colonised by emergent macrophytes within one or two decades and become a carbon sink as found for a deeply (1 m) flooded fen in southern Belarus (Minke *et al*. 2016). Continuous shallow flooding leads to low heterotrophic respiration from plant debris and peat, and supports rapid establishment of vascular plants typical of mires. In this ideal situation *GPP* quickly exceeds R_{eco} and the site may even become a net carbon sink during the first year after flooding. During the first years net carbon uptake may strongly exceed reported apparent carbon accumulation rates (LORCA) for northern peatlands (e.g. Botch 1995, Turunen *et al.* 2002, Gorham *et al.* 2003). However, the rate of carbon accumulation will certainly decrease over time as a new equilibrium between production, decay of organic matter and peat formation becomes established.

The response patterns of vegetation, carbon and GHGs to rewetting by beaver conform with those described from deliberate rewetting projects over longer periods of succession (Thiele *et al.* 2011, Minke *et al.* 2016). Water table drives vegetation development in rewetted fens. Fast, robust succession to potentially peat forming vegetation is key to a fast and strong transition to a net carbon sink and neutral GHG balance.

The role of the beaver in GHG mitigation depends on how its activities affect water table conditions. In contrast to deliberate peatland restoration projects designed to raise and stabilise water levels over the entire area, the fraction of land optimally rewetted by beaver will differ among peatlands and, especially in sloping areas, beaver dams may not be sufficient to keep water levels uniformly high (cf. Rakovich *et al.* 2003). Research is required on long-term developments, because beaver populations wax and wane so their dams may be maintained, extended or abandoned (Naiman *et al.* 1988). However, without beaver activity the water level in our study area at Barcianicha would have remained low and peat oxidation would have continued not only at the forbs site but also at the meadow sites.

Beavers are of great benefit in peatland restoration and a valuable support for the slowly progressing deliberate rewetting activities in Belarus and beyond. Related GHG emission reductions are relevant for the climate and should be reported under the United Nations Framework Convention on Climate Change (UNFCCC). Future studies should focus on the development of approaches to determine and monitor the spatially and temporally variable GHG fluxes of beaver-flooded areas, on the analysis of factors that are important for beaver population and activity, and on countrywide assessment of peatlands influenced by beavers.

ACKNOWLEDGEMENTS

This study was funded by the KfW Entwicklungsbank in the framework of the International Climate Initiative of the German Federal Ministry for the Environment, Nature Conservation and Nuclear Safety (BMU) under BMU project Reference No.: II. C. 53, and by the Centre for International Migration and Development (CIM) and the Royal Society for the ProteGünmction of Birds (RSPB). We thank: APB - BirdLife Belarus and the National Academy of Sciences of Belarus for creating ideal research conditions; the Michael Succow Foundation for their help with research equipment and logistics; Hans Joosten for support in designing the study and for commenting on the manuscript; Nadzeya Liashchynskaya, Hanna Grabenberger, Aleksandr Novik, Nikolaj Belovezhkin, Konstantin Timokhov and Aleksandr Pavlyuchenko for help in the field; Sergej Zui for construction and maintenance of measuring equipment; Vyacheslav Rakovich for showing us Barcianicha; Petr Boldovskij for the warm welcome, logistical support and information on land use history; Aleksandr Kozulin for site information; Roland Fuß for providing model scripts and consultations on statistical issues; and Michel Bechtold for advice on evaluation of the hydrological data. We also thank Stephan Glatzel and two anonymous reviewers for their valuable comments on the manuscript.

AUTHOR CONTRIBUTIONS

TY, AB, HH, VT and MM measured GHG emissions. MM calculated the fluxes including error calculations and analysed the data. JA advised on design, implementation and evaluation of measurements. AS provided data and text on vegetation, peat and water level. MM designed the manuscript with help from AF. MM wrote the draft and finalised the manuscript with the support of all authors.

REFERENCES

AG Boden (2005) *Bodenkundliche Kartieranleitung* (*Soil Mapping Manual*). 5th edition, Schweizerbart, Hannover, 438 pp. (in German).

Augustin, J., Chojnicki, B. (2008) Austausch von klimarelevanten Spurengasen, Klimawirkung und Kohlenstoffdynamik in den ersten Jahren nach der Wiedervernässung von degradiertem Niedermoorgrünland (Exchange of climate-relevant trace gases, climate effect and carbon dynamics in the first years after rewetting of degraded fen grassland). In: Gelbrecht J., Zak D., Augustin J. (eds.) *Phosphor- und Kohlenstoff-Dynamik und Vegetationsentwicklung in wiedervernässten Mooren des Peenetals in Mecklenburg-Vorpommern - Status, Steuergrößen und Handlungsmöglichkeiten (Phosphorus and Carbon Dynamics and Vegetation Development in Rewetted Fens of the Peene Valley in Mecklenburg-Western Pomerania - Status, Control Variables and Possibilities for Action)*. Berichte des IGB, 26, Leibniz-Institute of Freshwater Ecology and Inland Fisheries (IGB), Berlin, 50–67 (in German).

Bambalov, N., Tanovitskaya, N., Kozulin, A., Rakovich, V. (2017) Belarus. In: Joosten, H., Tanneberger, F., Moen, A. (eds.) *Mires and Peatlands of Europe: Status, Distribution and Conservation*. Schweizerbart, Stuttgart, 288–298.

Bartlett, K.B., Harriss, R.C. (1993) Review and assessment of methane emissions from wetlands. *Chemosphere*, 26, 261–320.

Beyer, C., Höper, H. (2015) Greenhouse gas exchange of rewetted bog peat extraction sites and a *Sphagnum* cultivation site in northwest Germany. *Biogeosciences*, 12, 2101–2117.

Botch, M.S., Kobak, K.I., Vinson, T.S., Kolchugina, T.P. (1995) Carbon pools and accumulation in peatlands of the Former Soviet Union, *Global Biogeochemical Cycles*, 9, 37–46.

Ciais, P., Sabine, C., Bala, G., Bopp, L., Brovkin, V., Canadell, J., Chhabra, A., DeFries, R., Galloway, J., Heimann, M., Jones, C., Le Quéré, C., Myneni, R.B, Piao, S., Thornton, P. (2013) Carbon and other biogeochemical cycles. In: Stocker, T.F., Qin, D., Plattner, G.-K., Tignor, M., Allen, S.K., Boschung, J., Nauels, A., Xia, Y., Bex, V., Midgley, P.M. (eds.) *Climate Change 2013: The Physical Science Basis. Contribution of Working Group I to the Fifth Assessment Report of the Intergovernmental Panel on Climate Change*. Cambridge University Press, Cambridge, United Kingdom and New York, NY, USA, 465–570.

Couwenberg, J., Thiele, A., Tanneberger, F., Augustin, J., Bärisch, S., Dubovik, D., Liashchynskaya, N., Michaelis, D., Minke, M., Skuratovich, A., Joosten, H. (2011) Assessing greenhouse gas emissions from peatlands using vegetation as a proxy. *Hydrobiologia*, 674, 67–89.

Dietrich, O., Kaiser, T. (2017) Impact of groundwater regimes on water balance components of a site with a shallow water table. *Ecohydrology*, 10 (e1867), 1–15.

Dise, N.B., Gorham, E., Verry, E.S. (1993) Environmental factors controlling methane emissions from peatlands in Northern Minnesota. *Journal of Geophysical Research*, 98, 10583–10594.

Drösler, M. (2005) *Trace Gas Exchange and Climatic Relevance of Bog Ecosystems, Southern Germany*. PhD thesis, Technische Universität München, Munich, 182 pp.

Drösler, M., Freibauer, A., Christensen, T.R., Friborg, T. (2008) Observations and status of peatland greenhouse gas emissions in Europe. In: Dolman, H., Valentini, R., Freibauer, A. (eds.) *The Continental-Scale Greenhouse Gas Balance of Europe*. Ecological Studies, 203, Springer, New York, 243–261.

Dušek, J., Žížková, H., Stellner, S., Czerný, R., Květ, J. (2012) Fluctuating water table affects gross ecosystem production and gross radiation use efficiency in a sedge-grass marsh. *Hydrobiologia*, 692, 57–66.

Efron, B. (1979) Bootstrap methods: Another look at the jackknife. *The Annals of Statistics*, 7, 1–26.

Elsgaard, L., Gorres, C.-M., Hoffmann, C.C., Blicher-Mathiesen, G., Schelde, K., Petersen, S.O. (2012) Net ecosystem exchange of CO_2 and carbon balance for eight temperate organic soils under agricultural management. *Agriculture, Ecosystems & Environment*, 162, 52-67.

Franz, D., Koebsch, F., Larmanou, E., Augustin, J., Sachs, T. (2016) High net CO_2 and CH_4 release at a eutrophic shallow lake on a formerly drained fen. *Biogeosciences*, 13, 3051–3070.

Gelbrecht, J., Rossoll, T., Zak, D. (2008) Untersuchungsgebiete im Peene- und Trebeltal sowie Referenzgebiete in Brandenburg und Nordwest-Polen (Research areas in the Peene- and Trebel valley and reference areas in Brandenburg and NW-Poland). In: Gelbrecht J., Zak D., Augustin J. (eds.) *Phosphor- und Kohlenstoff-Dynamik und Vegetationsentwicklung in wiedervernässten Mooren des Peenetals in Mecklenburg-Vorpommern - Status, Steuergrößen und Handlungsmöglichkeiten (Phosphorus and Carbon Dynamics and Vegetation Development in Rewetted Fens of the Peene Valley in Mecklenburg-Western Pomerania - Status, Control Variables and Possibilities for Action)*. Berichte des IGB, 26, Leibniz-Institute of Freshwater Ecology and

Inland Fisheries (IGB), Berlin, 20–39 (in German).

Gorham, E., Janssens, J.A., Glaser, P.H. (2003) Rates of peat accumulation during the postglacial period in 32 sites from Alaska to Newfoundland, with special emphasis on northern Minnesota. *Canadian Journal of Botany*, 81, 429–438.

Günther, A., Huth, V., Jurasinski, G., Glatzel, S. (2015) The effect of biomass harvesting on greenhouse gas emissions from a rewetted temperate fen. *Global Change Biology: Bioenergy*, 7, 1092–1106.

Gurnell, A.M. (1998) The hydrogeomorphological aspects of beaver dam-building activity. *Progress in Physical Geography*, 22, 167-189.

Hahn, J., Köhler, S., Glatzel, S., Jurasinski, G. (2015) Methane exchange in a coastal fen in the first year after flooding - A systems shift. *PLoS ONE*, 10 (e0140657), 1–25.

Hahn-Schöfl, M., Zak, D., Minke, M., Gelbrecht, J., Augustin, J., Freibauer, A. (2011) Organic sediment formed during inundation of a degraded fen grassland emits large fluxes of CH_4 and CO_2. *Biogeosciences*, 8, 1539–1550.

Halley, D.J., Rosell, F., Saveljev, A. (2012) Population and distribution of Eurasian beaver (Castor fiber). *Baltic Forestry*, 18, 168–175.

Hoffmann, M., Jurisch, N., Albiac Borraz, E.A., Hagemann, U., Drösler, M., Sommer, M., Augustin, J. (2015) Automated modeling of ecosystem CO_2 fluxes based on periodic closed chamber measurements: a standardized conceptual and practical approach. *Agricultural and Forest Meteorology*, 200, 30–45.

Huth, V., Vaidya, S., Hoffmann, M., Jurisch, N., Günther, A., Gundlach, L., Hagemann, U., Elsgaard, L., Augustin, J. (2017) Divergent NEE balances from manual-chamber CO_2 fluxes linked to different measurement and gap-filling strategies: A source for uncertainty of estimated terrestrial C sources and sinks? *Journal of Plant Nutrition and Soil Science*, 180, 302–315.

Ilina, M., Gurova, T. (2016) Ильина, М., Гурова, Т. Надежда на бобров, или Как на Полесье справляются с засухами (Hope for the beaver, or how Polessie is fighting with dryness). Interview at: http://greenbelarus.info/articles/17-06-2016/kak-bobry-pomogayut-spravitsya-s-problemoy-zasuh-na-polese, Brest Green Portal (in Russian).

Immirzi, C.P., Maltby, E., Clymo, R.S. (1992) *The Global Status of Peatlands and Their Role in Carbon Cycling.* Friends of the Earth, London, 145 pp.

IPCC (2014) *2013 Supplement to the 2006 IPCC Guidelines for National Greenhouse Gas Inventories: Wetlands*. Hiraishi, T., Krug, T., Tanabe, K., Srivastava, N., Baasansuren, J., Fukuda, M., Troxler, T.G. (eds.), IPCC, Switzerland, 354 pp.

IUSS Working Group WRB (2015) *World Reference Base for Soil Resources 2014, International Soil Classification System for Naming Soils and Creating Legends for Soil Maps, Update 2015.* World Soil Resources Reports No. 106. FAO, Rome, 203 pp.

Joosten, H. (2009) *The Global Peatland CO_2 Picture. Peatland Status and Emissions in All Countries of the World*. Wetlands International, Ede, 35 pp.

Joosten, H., Sirin, A., Couwenberg, J., Laine, J., Smith, P. (2016) The role of peatlands in climate regulation. In: Bonn, A., Allott, T., Evans, M., Joosten, H., Stoneman, R. (eds.) *Peatland Restoration and Ecosystem Services: Science, Policy and Practice*. Cambridge University Press/ British Ecological Society, Cambridge, 63–76.

Joosten, H., Tapio-Biström, M.-L., Tol, S. (eds.) (2012) *Peatlands - Guidance for Climate Change Mitigation through Conservation, Rehabilitation and Sustainable Use*. Mitigation of Climate Change in Agriculture (MICCA) Programme, FAO/Wetlands International, Rome, 100 pp.

Jurasinski, G., Koebsch, F., Hagemann, U. (2012) Flux: Flux rate calculation from dynamic closed chamber measurements. R Package Version 0.2-1, Rostock. Online at: http://cran.r-project.org/web/packages/flux

Karran, D.J. (2018) *The Engineering of Peatland Form and Function by Beaver (Castor spp.)*. PhD thesis, University of Saskatchewan, Saskatoon, 139 pp.

Köppen, W. (1936) Das geographische System der Klimate. In: Köppen, W., Geiger, R. (eds.) *Handbuch der Klimatologie (Handbook of Climatology)*, 1(C). Borntraeger, Berlin, 44 pp. (in German).

Koska, I., Succow, M., Clausnitzer, U., Timmermann, T., Roth, S. (2001) Vegetationskundliche Kennzeichnung von Mooren (topische Betrachtung) (Characterisation of mires by vegetation (topical observation)). In: Succow, M., Joosten, H. (eds.) *Landschaftsökologische Moorkunde (Landscape Ecology of Mires)*. Schweizerbart, Stuttgart, 112–184 (in German).

Kottek, M., Grieser, J., Beck, C., Rudolf, B., Rubel, F. (2006) World map of the Köppen-Geiger climate classification up–dated. *Meteorologische Zeitschrift*, 15, 259–263.

Kozulin, A., Tanovitskaya, N., Vershitskaya, I.

(2010) *Methodical Recommendations for Ecological Rehabilitation of Damaged Mires and Prevention of Disturbance to the Hydrological Regime of Mire Ecosystems in the Process of Drainage*. ALTIORA-Live Colours, Minsk, 40 pp.

Lamers, L.P.M., Smolders, A.J.P., Roelofs, J.G.M. (2002) The restoration of fens in the Netherlands. *Hydrobiologia*, 478, 107–130.

Law, A., Gaywood, M., Jones, K.C., Ramsay, P., Willby, N.J. (2017) Using ecosystem engineers as tools in habitat restoration and rewilding: beaver and wetlands. *Science of the Total Environment*, 605–606, 1021–1030.

Leiber-Sauheitl, K., Fuß, R., Voigt, C., Freibauer, A. (2014) High CO_2 fluxes from grassland on histic Gleysol along soil carbon and drainage gradients. *Biogeosciences*, 11, 749–761.

Leiber-Sauheitl, K., Fuß, R., Lempio, D., Tiemeyer, B., Bechtold, M., Freibauer, A. (2015) Minimum measurement frequency for robust annual budgets of ecosystem respiration. In: Sauheitl, K. *Shallow Organic Soils as Significant Greenhouse Gas Sources*. PhD thesis, Universität Hannover, Hannover, 27–53.

Leifeld, J., Menichetti, L. (2018) The underappreciated potential of peatlands in global climate change mitigation strategies. *Nature Communications*, 9 (1071), 1–7.

Lloyd, J., Taylor, J.A. (1994) On the temperature dependence of soil respiration. *Functional Ecology*, 8, 315–323.

Maksimenkov, M.V., Pugachevskij, A.V., Rakovich, V.A. (2006) *Научное Обоснование Повторного Заболачивания Выработанного Торфяного Месторождения "Бортениха" (Scientific Justification of Rewetting of the Cutaway Peatland "Bortenikha")*. The Forest Ministry of the Republic of Belarus, Minsk, 38 pp. (in Russian).

Meyer, K. (1999) *Die Flüsse der klimarelevanten Gase CO_2, CH_4 und N_2O eines nordwestdeutschen Niedermoores unter dem Einfluss der Wiedervernässung (Fluxes of the greenhouse gases CO_2, CH_4 und N_2O from a Fen in NW-Germany after Rewetting)*. Göttinger Bodenkundliche Berichte, 111, Georg-August-Universität, Göttingen, 135 pp. (in German).

Michaelis, L., Menten, M. L. (1913) Die Kinetik der Invertinwirkung. *Biochemische Zeitschrift*, 49, 333–369.

Minke, M., Augustin, J., Burlo, A., Yarmashuk, T., Chuvashova, H., Thiele, A., Freibauer, A., Tikhonov, V., Hoffmann, M. (2016) Water level, vegetation composition, and plant productivity explain greenhouse gas fluxes in temperate cutover fens after inundation, *Biogeosciences*, 13, 3945–3970.

Mitchell, C.C., Niering, W.A. (1993) Vegetation change in a topogenic bog following beaver flooding. *Bulletin of the Torrey Botanical Club*, 120, 136–147.

Moore, P.D., Bellamy, D.J. (1974) *Peatlands*. Elek Science, London, 221 pp.

Moore, T.R., Dalva, M. (1993) The influence of temperature and water table position on carbon dioxide and methane emissions from laboratory columns of peatland soils. *Journal of Soil Science*, 44, 651–664.

Moriasi, D.N., Arnold, J.G., Van Liew, M.W., Binger, R.L., Harmel, R.D., Veith, T. (2007) Model evaluation guidelines for systematic quantification of accuracy in water-shed simulations. *American Society of Agricultural and Biological Engineers*, 50, 885–900.

Morrison, A., Westbrook, C.J., Bedard-Haughn, A. (2015) Distribution of Canadian Rocky Mountain wetlands impacted by beaver. *Wetlands*, 35, 95–104.

Myhre, G., Shindell, D., Bréon, F.-M., Collins, W., Fuglestvedt, J., Huang, J., Koch, D., Lamarque, J.-F., Lee, D., Mendoza, B., Nakajima, T., Robock, A., Stephens, G., Takemura, T., Zhang, H. (2013) Anthropogenic and natural radiative forcing. In: Stocker, T.F., Qin, D., Plattner, G.-K., Tignor, M., Allen, S.K., Boschung, J., Nauels, A., Xia, Y., Bex, V., Midgley, P.M. (eds.) *Climate Change 2013: The Physical Science Basis, Contribution of Working Group I to the Fifth Assessment Report of the Intergovernmental Panel on Climate Change*. Cambridge University Press, Cambridge, UK, New York, NY, USA, 659–740.

Naiman, R., Johnston, C., Kelley, J. (1988) Alteration of North American streams by beaver. *BioScience*, 38, 753–762.

Page, S.E., Rieley, J.O., Banks, C.J. (2011) Global and regional importance of the tropical peatland carbon pool. *Global Change Biology*, 17, 798–818.

Patterson, L., Cooper, D.J. (2007) The use of hydrologic and ecological indicators for the restoration of drainage ditches and water diversions in a Mountain Fen, Cascade Range, California. *Wetlands*, 27, 290–304.

Peet, R.K., Wentworth, T.R., White, P.S. (1998) A flexible, multipurpose method for recording vegetation composition and structure. *Castanea*, 63, 262–274.

Rakovich, V.A., Bambalov, N.N. (1996) Особенности функционирования

выработанных торфяных месторождений в биосфере (Characteristics of the functioning of extracted peatlands in the biosphere). *Природопользование* (*Nature management*), 1, 158–163 (in Russian).

Rakovich, V.A., Smirnova, V.V., Ivkovich, V.S. (2003) Закономерности восстано-вления болотообразовательного процесса на выработанных торфяных месторождениях водораздельного залегания (на примере торфяного месторождения Зеликов Мох) (Regularities of the restoration of the peat forming process in extracted peatlands of the watershed (on the example of the peatland Zelikov Mokh)). *Природопользование* (*Nature management*), 9, 14–19 (in Russian).

Rothmaler, W. (2000) *Exkursionsflora von Deutschland, Band 3, Gefäßpflanzen: Atlasband (Excursion Flora of Germany, Volume 3, Vascular Plants)*. 10th edition, Spektrum Akademischer Verlag GmbH Heidelberg, Berlin, 753 pp. (in German).

Roulet, N.T., Crill, P., Comer, N. (1997) CO_2 and CH_4 flux between a boreal beaver pond and the atmosphere. *Journal of Geophysical Research*, 102 (D24), 29,313–29,319.

Samaritani, E., Siegenthaler, A., Yli-Petäys, M., Buttler, A., Christin, P.-A., Mitchell, E.A.D. (2011) Seasonal net ecosystem carbon exchange of a regenerating cutaway bog: how long does it take to restore the C-sequestration function? *Restoration Ecology*, 19, 480–489.

Sirin, A., Minayeva, T., Yurkovskaya, T., Kuznetsiv, O., Smagin, V., Fedotov, Y. (2017) Russian Federation (European Part). In: Joosten, H., Tanneberger, F., Moen, A. (eds.) *Mires and Peatlands of Europe: Status, Distribution and Conservation*. Schweizerbart, Stuttgart, 589–616.

Strachan, I.B., Nugent, K.A., Crombie, S., Bonneville, M.-C. (2015) Carbon dioxide and methane exchange at a cool-temperate freshwater marsh. *Environmental Research Letters*, 10 (065006), 1–10.

Succow, M., Stegmann, H., Zeitz, J., Koska, I. (2001) Abiotische Kennzeichnung von Moorstandorten (topische Betrachtung) (Abiototic characterisation of peatland sites (topical observation)). In: Succow, M., Joosten, H. (eds.), *Landschaftsökologische Moorkunde (Landscape Ecology of Mires)*. Schweizerbart, Stuttgart, 58–111 (in German).

Tanneberger, F., Joosten, H., Moen, A., Whinam, J. (2017) Mire and peatland conservation in Europe. In: Joosten, H., Tanneberger, F., Moen, A. (eds.) *Mires and Peatlands of Europe: Status, Distribution and Conservation*. Schweizerbart, Stuttgart, 173–196.

Tanneberger, F., Thiele, A. (2011) Practical rewetting examples: Introduction. In: Tanneberger, F., Wichtmann, W. (eds.) *Carbon Credits from Peatland Rewetting: Climate - Biodiversity - Land Use*. Schweizerbart, Stuttgart, p. 169.

Thiele, A., Edom, F., Liashchynskaya, N. (2011) Prediction of vegetation development with and without rewetting. In: Tanneberger, F., Wichtmann, W. (eds.) *Carbon Credits from Peatland Rewetting: Climate - Biodiversity - Land Use*. Schweizerbart, Stuttgart, 42–52.

Timmermann, T., Margóczi, K., Takács, G., Vegelin, K. (2006) Restoration of peat-forming vegetation by rewetting species-poor fen grasslands. *Applied Vegetation Science*, 9, 241–250.

Tokida, T., Mizoguchi, M., Miyazaki, T., Kagemoto, A., Nagata, O., Hatano, R. (2007) Episodic release of methane bubbles from peatland during spring thaw. *Chemosphere*, 70, 165–171.

Turunen, J., Tomppo, E., Tolonen, K., Reinikainen, A. (2002) Estimating carbon accumulation rates of undrained mires in Finland: Application to boreal and subarctic regions. *Holocene*, 12, 69–80.

Voitekhovitch, I., Chabrouskaya, O., Thiele, A., Tanneberger, F. (2011a) Practical rewetting example: Dakudauskaje. In: Tanneberger, F., Wichtmann, W. (eds.) *Carbon Credits from Peatland Rewetting: Climate - Biodiversity - Land Use*. Schweizerbart, Stuttgart, 181–183.

Voitekhovitch, I., Chabrouskaya, O., Thiele, A., Tanneberger, F. (2011b) Practical rewetting example: Dalbeniski. In: Tanneberger, F., Wichtmann, W. (eds.) *Carbon Credits from Peatland Rewetting: Climate - Biodiversity - Land Use*. Schweizerbart, Stuttgart, 170–172.

Wickland, K., Striegl, R.G., Mast, M.A., Clow, D.W. (2001) Carbon gas exchange at a southern Rocky Mountain wetland, 1996–1998. *Global Biogeochemical Cycles*, 15, 321–335.

Wilson, D., Farrell, C., Mueller, C., Hepp, S., Renou-Wilson, F. (2013) Rewetted industrial cutaway peatlands in western Ireland: a prime location for climate change mitigation? *Mires and Peat*, 11 (01), 1–22.

Wilson, D., Blain, D., Couwenberg, J., Evans, C.D., Murdiyarso, D., Page, S.E., Renou-Wilson, F., Rieley, J.O., Sirin, A., Strack, M., Tuittila, E.-S. (2016) Greenhouse gas emission factors associated with rewetting of organic soils. *Mires and Peat*, 17 (04) 1–28.

Woo, M., Waddington, J.M. (1990) Effects of beaver

dams on subarctic wetland hydrology. *Arctic*, 43, 223–230.

Zerbe, S., Steffenhagen, P., Parakenings, K., Timmermann, T., Frick, A., Gelbrecht, J., Zak, D. (2013) Ecosystem service restoration after 10 years of rewetting peatlands in NE Germany. *Journal of Environmental Management*, 51, 1194–1209.

Zhuravlev, D., Tanneberger, T. (2011) Experience from rewetted sites in Belarus – Chernobyl zone. In: Tanneberger, F., Wichtmann, W. (eds.) *Carbon Credits from Peatland Rewetting: Climate - Biodiversity - Land Use*. Schweizerbart, Stuttgart, p. 72.

Submitted 20 May 2019, final revision 21 Jun 2020
Editor: Stephan Glatzel

Author for correspondence: Merten Minke, Institute of Botany and Landscape Ecology, University of Greifswald, partner in the Greifswald Mire Centre, Soldmannstraße 15, D-17487 Germany.
Tel: +49 1577 4184844; E-Mail: mertenchristian@gmx.de

Appendix

Table A1. Plant species cover of GHG measuring plots. Plant cover scale according to Peet *et al.* (1998): 1 = very few individuals, 2 = cover of 0–1 %, 3 = 1–2 %, 4 = 2–5 %, 5 = 5–10 %, 6 = 10–25 %, 7 = 25–50 %, 8 = 50–75 %, 9 = 75–95 %, 10 ≥ 95 %. Tree species are given individually for herb layer (h; 0-40cm), shrub layer (sh; 40–200cm) and tree layer (t; >200cm). *Deeply flooded meadow* was free of living plants in 2010.

	Shallowly flooded forbs									*Shallowly flooded meadow*									*Deeply flooded meadow*								
species	Jul 2010			Nov 2011			Jun 2012			Jul 2010			Nov 2011			Jun 2012			Jul 2010			Nov 2011			Jun 2012		
	I	II	III	I	II	III	I	II	III	I	II	III	I	II	III	I	II	III	I	II	III	I	II	III	I	II	III
Urtica dioica	8	7	6																								
Galeopsis tetrahit	1																										
Poa trivialis	7	6	10		1	8			2																		
Cirsium arvense	5		1																								
Cardaminopsis arenosa	1		1																								
Erysimum cheiranthoides		1	1																								
Potentilla norvegica	2																										
Cirsium oleraceum			1																								
Galium mollugo			1																								
Campylium polygamum	7	8							6							2	3	3									
Equisetum				1																							
Iris pseudacorus						1																					
Lemna trisulca									2																		
Utricularia intermedia									4																		
Agrostis stolonifera										6	7	6		2	2												
Equisetum palustre										2	3	2															

	Shallowly flooded forbs									*Shallowly flooded meadow*									*Deeply flooded meadow*								
species	Jul 2010			Nov 2011			Jun 2012			Jul 2010			Nov 2011			Jun 2012			Jul 2010			Nov 2011			Jun 2012		
	I	II	III	I	II	III	I	II	III	I	II	III	I	II	III	I	II	III	I	II	III	I	II	III	I	II	III
Elytrigia repens										4	3																
Dicranella heteromalla										2																	
Fallopia convolvulus											1																
Rumex sanguineus										1		1															
Salix cinerea											h2																
Salix pentandra												h1															
Taraxacum officinale												1															
Potentilla anserina										4	5	3		1													
Lycopus europaeus											1	1	2	4		3	2										
Mentha aquatica														1													
Carex rostrata													7			8											
Carex pseudocyperus													1	2			1										
Chara																2	2	2									
Equisetum fluviatile																	1										
Juncus articulatus									2				1	3	2	2	3	1									
Bidens frondosa									4				3				1										
green algae							5	8	4					3	2	4	3	3									
Typha latifolia						1			5									1									
Alisma plantago-aquatica								2	1				1	1	4	4	7	7				1			4		
Lemna minor				1		5		2	5				2	2		2	2	2							1	2	2
Lythrum salicaria								1														1					
Chara vulgaris																						5	8		8	10	7

Table A2. Nash–Sutcliffe efficiency (NSE) of CO_2 and CH_4 models calibration and leave-one-out cross validation. NSE values between 0.0 and 1.0 are acceptable, but values < 0.0 indicate unacceptable model performance (Moriasi *et al.* 2007).

Site	Year	Plot	Calibration, NSE			Validation, NSE		
			R_{eco}	*NEE*	CH_4	R_{eco}	*NEE*	CH_4
Deeply flooded meadow	1	I	0.60	0.60	0.47	-0.74	-0.74	0.42
		II	0.59	0.59		-1.15	-1.15	
		III	0.67	0.67		-0.88	-0.88	
	2	I	0.75	0.64	0.13	-0.07	0.30	0.01
		II	0.74	0.74		0.38	0.42	
		III	0.79	0.68		0.32	0.45	
Shallowly flooded meadow	1	I	0.97	0.94	0.33	0.07	0.38	0.31
		II	0.98	0.96		-0.04	0.46	
		III	0.98	0.95		0.07	0.23	
	2	I	0.97	0.91	0.29	0.44	0.63	0.18
		II	0.92	0.95		0.42	0.62	
		III	0.95	0.97		0.44	0.32	
Shallowly flooded forbs	1	I	0.95	0.86	-	-0.75	-0.30	-
		II	0.91	0.72		-0.89	-1.44	
		III	0.94	0.69		-0.25	-1.19	
	2	I	0.90	0.92	-	0.24	0.21	-
		II	0.83	0.87		0.49	0.58	
		III	0.95	0.51		0.66	0.27	